TTP 94-28
November 1994
hep-ph/9411395

Polarization in Top Quark Pair Production near Threshold *†

R. Harlander[a], M. Ježabek[a,b], J.H. Kühn[a] and T. Teubner[a]

[a] *Institut für Theoretische Teilchenphysik, D-76128 Karlsruhe, Germany*

[b] *Institute of Nuclear Physics, Kawiory 26a, PL-30055 Cracow, Poland*

Abstract

The polarization dependent momentum distributions of top quarks and their decay products are calculated for $t\bar{t}$ production at future e^+e^- colliders with polarized beams. The Green function formalism is applied to this reaction near energy threshold. The Lippmann–Schwinger equations for the S-wave and P-wave Green functions are solved numerically for the QCD chromostatic potential given by the two-loop formula at large momentum transfers and Richardson ansatz at intermediate and small ones. It is demonstrated that for the longitudinally polarized electron beam an optimally polarized sample of top quarks can be produced.

*Work supported in part by KBN grant 2P30225206, by BMFT contract 056KA93P and by DFG contract 436POL173193S.

†The complete paper, including figures, is also available via anonymous ftp at ttpux2.physik.uni-karlsruhe.de (129.13.102.139) as /ttp94-28/ttp94-28.ps, or via www at http://ttpux2.physik.uni-karlsruhe.de/preprints.html/

Introduction

There is no doubt that precise studies of top quark interactions will lead to profound progress in particle physics. The top quark is the heaviest fermion of the Standard Model. Its large mass allows to probe deeply into the QCD potential for nonrelativistic $t\bar{t}$ system produced near threshold. Such a system will provide a unique opportunity for a variety of novel QCD studies. Polarization studies for $t\bar{t}$ pairs near threshold are free from hadronization ambiguities. This is due to the short lifetime of the top quark. The lifetime of the top quark is shorter than the formation time of top mesons and toponium resonances. Therefore top decays intercept the process of hadronization at an early stage and practically eliminate associated nonperturbative effects.

The analysis of polarized top quarks and their decays has recently attracted considerable attention (See [1, 2] and references cited therein). The reason is that this analysis will result in determination of the top quark coupling to the W and Z bosons either confirming the predictions of the Standard Model or providing clues for physics beyond. The latter possibility is particularly intriguing because m_t plays an exceptional role in the fermion mass spectrum.

A number of mechanisms have been suggested that will lead to polarized top quarks. However, studies at a linear electron-positron collider are particularly clean for precision tests. Moreover, close to threshold and with longitudinally polarized electrons one can study decays of polarized top quarks under particularly convenient conditions: large event rates, well-identified rest frame of the top quark, and large degree of polarization. At the same time, thanks to the spectacular success of the polarization program at SLC [3], the longitudinal polarization of the electron beam will be an obvious option for a future linear collider[1].

In the present article[2] top quark polarization is studied in the reaction $e^+e^- \to t\bar{t}$. The calculations of top polarization well above the threshold for $t\bar{t}$ production were published long ago [7]. The threshold region, however, deserves a special study. To demonstrate that this polarization is indeed experimentally accessible we review briefly polarization effects in top decays.

[1]Another proposed and closely related facility is a photon linear collider. At such a machine the high energy photon beams can be generated via Compton scattering of laser light on electrons accelerated in the linac. The threshold behaviour of the reaction $\gamma\gamma \to t\bar{t}$ has been reviewed in [4] and the top quark polarization in this reaction has been recently considered in [5].

[2]Some results of these studies have been presented in [6].

Subsequently we discuss the dependence of the top quark polarization on the longitudinal polarizations of the beams. Due to restricted phase space the amplitude is dominantly S wave and the electron and positron polarizations are directly transferred to the top quark. For a quantitative study this simple picture has to be extended and the modifications originating from $S-P$ wave interference should be taken into account. As a consequence of final state interaction between t and $\bar{t}$, which leads to the familiar QCD potential, the parton model prediction where these terms are simply proportional to $\beta=\sqrt{1-4m_t^2/s}$ has to be modified. The interference terms are therefore calculated from numerical solutions of Lippmann-Schwinger equations.

Decays of polarized top quarks

The polarization four-vector s^μ of the top quark can be determined from the angular-energy distributions of the charged leptons in semileptonic t decays. In the t quark rest frame this distribution is in Born approximation the product of the energy and the angular distributions [8]:

$$\frac{\mathrm{d}^2\Gamma}{\mathrm{d}E_\ell\,\mathrm{d}\cos\theta}=\frac{1}{2}\left[1\,+\,S\cos\theta\right]\frac{\mathrm{d}\Gamma}{\mathrm{d}E_\ell} \tag{1}$$

where $s^\mu=(0,\vec{s}\,)$, $S=|\,\vec{s}\,|$ and θ is the angle between $\vec{s}$ and the direction of the charged lepton. QCD corrections essentially do not spoil factorization [9]. Thus, the polarization analyzing power of the charged lepton energy-angular distribution remains maximal. There is no factorization for the neutrino energy-angular distribution which is therefore less sensitive to the polarization of the decaying top quark. On the other hand it has been shown [10] that the angular-energy distribution of neutrinos from the polarized top quark decay will allow for a particularly sensitive test of the V-A structure of the weak charged current.

Top polarization at a linear collider

We adopt the conventions of ref.[11] and describe the longitudinal polarization of the e^+e^- system in its center-of-mass frame as a function of the variable

$$\chi=\frac{P_{e^+}-P_{e^-}}{1-P_{e^+}P_{e^-}} \tag{2}$$

where $P_{e^\pm}$ denote the polarizations of $e^\pm$ with respect to the directions of e^+

and e^- beams, respectively[3]. A righthanded system of coordinates is defined through the triplet of othogonal unit vectors: $\hat{n}_\perp$, $\hat{n}_N$ and $\hat{n}_\parallel$ where $\hat{n}_\parallel$ points in the direction of e^- beam, $\hat{n}_N \sim \vec{p}_{e^-} \times \vec{p}_t$ is normal to the production plane and $\hat{n}_\perp = \hat{n}_N \times \hat{n}_\parallel$. In the absence of phases from final state interaction, which can be induced by higher orders in α_s and will be considered elsewhere, the top quark polarization vector is in the production plane and $P_\parallel$ and $P_\perp$ denote its longitudinal and transverse components. The definition of $P_\parallel$ and $P_\perp$ with respect to the beam direction is convenient for the treatment close to threshold and differs from the definition of [7] where the quantities have been defined with respect to the direction of flight of the top quark. The angle ϑ denotes the angle between e^- and the top quark.

In the threshold region the top quark is nonrelativistic (with velocity $\beta = p/m_t \sim \alpha_s$) and the kinetic energy of the $t\bar{t}$ system $E = \sqrt{s} - 2m_t$ is of order $\mathcal{O}(\beta^2)$. As a consequence of the $t\bar{t}$ interaction the top quarks will exhibit a momentum spread (Fermi motion) even for fixed energy E [12]. Also the polarization and the angular distribution will depend on both E and p. Retaining only the terms up to $\mathcal{O}(\beta)$ one derives the following expressions for the components of the polarization vector, as functions of E, p and ϑ

$$\begin{aligned} \mathcal{P}_\parallel(p,E,\vartheta) &= C_\parallel^0(\chi) + C_\parallel^1(\chi)\varphi(p,E)\cos\vartheta & (3)\\ \mathcal{P}_\perp(p,E,\vartheta) &= C_\perp(\chi)\varphi(p,E)\sin\vartheta & (4) \end{aligned}$$

and, after the integration over top quark momentum p,

$$\begin{aligned} P_\parallel(E,\vartheta) &= C_\parallel^0(\chi) + C_\parallel^1(\chi)\Phi(E)\cos\vartheta & (5)\\ P_\perp(E,\vartheta) &= C_\perp(\chi)\Phi(E)\sin\vartheta & (6) \end{aligned}$$

where

$$\begin{aligned} C_\parallel^0(\chi) &= -\frac{a_2 + \chi a_1}{a_1 + \chi a_2} & (7)\\ C_\parallel^1(\chi) &= -(1-\chi^2)\frac{a_1 a_4 - a_2 a_3}{(a_1 + \chi a_2)^2} & (8)\\ C_\perp(\chi) &= -\frac{1}{2}\frac{a_4 + \chi a_3}{a_1 + \chi a_2} & (9) \end{aligned}$$

[3]It is conceivable that for a future linear e^+e^- collider $P_{e^+} = 0$, $P_{e^-} \neq 0$ and then $\chi = -P_{e^-}$.

with

$$
\begin{aligned}
a_1 &= q_e^2 q_t^2 + (v_e^2 + a_e^2) v_t^2 d^2 + 2 q_e q_t v_e v_t d \\
a_2 &= 2 v_e a_e v_t^2 d^2 + 2 q_e q_t a_e v_t d \\
a_3 &= 4 v_e a_e v_t a_t d^2 + 2 q_e q_t a_e a_t d \\
a_4 &= 2 (v_e^2 + a_e^2) v_t a_t d^2 + 2 q_e q_t v_e a_t d \\
d &= \frac{1}{16 \sin^2\theta_W \cos^2\theta_W} \frac{s}{s - M_Z^2}
\end{aligned}
$$

and

$$
\begin{array}{lll}
q_e = -1 & v_e = -1 + 4\sin^2\theta_W & a_e = -1 \\
q_t = \frac{2}{3} & v_t = 1 - \frac{8}{3}\sin^2\theta_W & a_t = 1
\end{array}
$$

The coefficients $C_\parallel^0(\chi)$, $C_\parallel^1(\chi)$ and $C_\perp(\chi)$ depend on the polarization χ, the electroweak coupling constants, the Z mass and the center-of-mass energy $\sqrt{s} \approx 2m_t$. They are plotted in Fig.1 for $m_t = 174$ GeV, $\sin^2\theta_W = 0.2317$ and $M_Z = 91.1888\ GeV$. $C_\parallel^0(\chi)$ and $C_\parallel^1(\chi)$ are shown in Fig.1a as the solid and the dashed lines, respectively, and $C_\perp(\chi)$ as the solid line in Fig.1b. Eqs.(3) and (4) extend the results of [7, 13] into the threshold region.

The functions $\varphi(p,E)$ and $\Phi(E)$ in eqs.(3)–(6) replace the simple factor β in a calculation for free, noninteracting quarks. They describe the complicated dynamics of the $t\bar{t}$ system near threshold which in particular includes effects of the would-be toponium resonances and Coulomb enhancement. Nevertheless, it is possible to calculate these functions using the Green function method. The same functions $\varphi(p,E)$ and $\Phi(E)$ also govern the angular distributions of the top quark in $e^+e^- \to t\bar{t}$. For fixed E and p the angular distribution is given by

$$
\frac{\mathrm{d}\mathcal{N}}{\mathrm{d}\cos\vartheta}(p,E) \sim (a_1 + \chi a_2) \; + \; (a_3 + \chi a_4)\; \varphi(p,E) \cos\vartheta \tag{10}
$$

and the corresponding forward-backward asymmetry reads

$$
\mathcal{A}_{FB}(p,E) \; = \; \int_0^1 \mathrm{d}\cos\vartheta \frac{\mathrm{d}\mathcal{N}}{\mathrm{d}\cos\vartheta} - \int_{-1}^0 \mathrm{d}\cos\vartheta \frac{\mathrm{d}\mathcal{N}}{\mathrm{d}\cos\vartheta} \; = \; C_{FB}(\chi)\, \varphi(p,E) \tag{11}
$$

The function

$$
C_{FB}(\chi) = \frac{1}{2} \frac{a_3 + \chi a_4}{a_1 + \chi a_2} \tag{12}
$$

is shown as the dashed line in Fig.1b. Integrating the distribution (10) over p one obtaines the forward-backward asymmetry

$$A_{FB}(E) = C_{FB}(\chi)\Phi(E) \tag{13}$$

which has been first obtained in [14] for $\chi = 0$.

Lippmann-Schwinger equations

To evaluate the functions $\varphi(p, E)$ and $\Phi(E)$ the Green function method is adequate which has become a standard tool for studying e^+e^- annihilation in the threshold region [15, 16, 17, 18]. We follow the momentum space approach [18] and solve the Lippmann-Schwinger equations numerically for the S-wave and P-wave Green functions

$$G(p,E) = G_0(p,E) + G_0(p,E)\int \frac{\mathrm{d}^3 q}{(2\pi)^3}\tilde{V}\left(\,|\vec{p}-\vec{q}|\,\right)G(q,E) \tag{14}$$

$$F(p,E) = G_0(p,E) + G_0(p,E)\int \frac{\mathrm{d}^3 q}{(2\pi)^3}\frac{\vec{p}\cdot\vec{q}}{p^2}\tilde{V}\left(\,|\vec{p}-\vec{q}|\,\right)F(q,E) \tag{15}$$

where $p = |\,\vec{p}\,|$ is the momentum of the top quark in $t\bar{t}$ rest frame,

$$G_0(p,E) = \Big(E - p^2/m_t + \mathrm{i}\Gamma_t\Big)^{-1} \tag{16}$$

and Γ_t denotes the top width. The QCD potential in momentum space $\tilde{V}(p)$ is described in [20].

In the nonrelativistic approximation the momentum distribution of the top quark is dominated by the S-wave contribution and it is proportional to

$$\mathcal{D}_{S-S}(p,E) = p^2\,|\,G\,|^2 \tag{17}$$

which is shown in Fig.2a. For $E = -2.6$ GeV (dashed line) $\mathcal{D}_{S-S}$ is relatively wide and exhibits the shape expected for the ground state wave function. For $E = 1$ GeV (solid line) the distribution becomes narrower and is peaked at a nonvanishing momentum corresponding to open top production. Contributions of $\mathcal{O}(\beta)$ to $\mathcal{P}_{\parallel}$ and $\mathcal{P}_{\perp}$ as well as to the forward-backward asymmetry $\mathcal{A}_{FB}$ arise from the interference of S- and P- waves and are therefore proportional to

$$\mathcal{D}_{S-P}(p,E) = p^3\,\mathcal{R}e\,(\,G\,F^*\,)\,/m_t \tag{18}$$

This distribution, shown in Fig.2b exhibits a significantly wider spread in momentum, a feature naturally explained by the larger momentum of P-states. The angular distribution (10), the forward-backward asymmetry (11), and the components (3) and (4) of the polarization vector for fixed E and p are then governed by the ratio

$$\varphi(p,E) = \frac{\left(1-\frac{4\alpha_s}{3\pi}\right)\,\mathcal{D}_{S-P}(p,E)}{\left(1-\frac{8\alpha_s}{3\pi}\right)\mathcal{D}_{S-S}(p,E)} \tag{19}$$

which is plotted in Fig.2c. The factors $\left(1-\frac{4\alpha_s}{3\pi}\right)$ and $\left(1-\frac{8\alpha_s}{3\pi}\right)$ originate from transversal gluon exchange [19]. In a similar way the function

$$\Phi(E) = \frac{\left(1-\frac{4\alpha_s}{3\pi}\right)\int_0^{p_m}\,\mathrm{d}p\,\mathcal{D}_{S-P}(p,E)}{\left(1-\frac{8\alpha_s}{3\pi}\right)\int_0^{p_m}\,\mathrm{d}p\,\mathcal{D}_{S-S}(p,E)} \tag{20}$$

describes the integrated quantities. The upper limit p_m has been introduced in order to cut off the logarithmic divergence of the numerator. The denominator remains finite for $p_m \to \infty$. In experimental analyses the contributions of very large intrinsic momenta will be automatically suppressed by the separation of $t\bar{t}$ events from the background. In our calculation we use $p_m = m_t/3$. The function $\Phi(E)$ is plotted in Fig.3a for $m_t = 174$ GeV. The QCD potential depends on $\alpha_s(m_Z)$ and our results are presented for $\alpha_s = 0.11\,/\,0.12\,/\,0.13$ as dotted/solid/dashed lines. For a comparison in Fig.3b the annihilation cross section $\sigma(e^+e^- \to t\bar{t})$ is shown in units of $\sigma(e^+e^- \to \mu^+\mu^-)$. The increase of $\Phi(E)$ with E resembles qualitatively the behaviour $\beta \approx \sqrt{E/m_t}$ expected for noninteracting quarks. Linear terms in β amount to typically 0.1 and could, therefore, be accessible experimentally, whereas relativistic corrections $\sim \beta^2$ are evidently small.

Combining Figs.(1)–(3) the predictions for the polarizations and the angular distributions can be discussed easily. The coefficient $C_\parallel^0(\chi)$ governs the leading term for the longitudinal polarization. (For electroweak corrections to this quantity see [21, 22].) For $\chi = \pm 1$ the top quark polarization is simply given by the polarization of the incoming electrons, resulting in $C_\parallel^0(\chi) = \mp 1$ and $C_\parallel^1(\chi) = 0$, and consequently in a nearly completely polarized sample of top quarks, *a strong argument for top production with polarized beams.* The deviation from the $\beta = 0$ prediction for the longitudinal top polarization is maximal at $\chi \approx -0.4$, where $C^0_\parallel(\chi)$ happens to vanish, but remains generally small. The coefficient $C_\perp(\chi)$ is small for unpolarized beams. For $\chi = -1$ however, it amounts to 0.65 which leads to sizeable polarization of top quarks perpendicular to the beam, if they are produced at large angles. The angular distribution and the forward-backward asymmetry A_{FB}, on the other hand, are fairly insensitive towards beam polarization in the threshold region. They can be used for experimental determination of $\Phi(E)$ which will test the QCD description of $t\bar{t}$ interactions and may lead to an independent determination of m_t and α_s.

Summary

Top quark polarization can be reliably predicted in the threshold region. Employing longitudinally polarized beams an optimally polarized sample of top quarks may be produced, allowing for precision studies of tbW coupling. Small corrections of order β arise from the admixture of P waves. These can be calculated using Green function techniques. The predictions are sensitive towards the potential model, leading to additional constraints on the value of α_s.

References

[1] J.H. Kühn, "Top Quark at a Linear Collider", in *Physics and Experiments with Linear e^+e^- Colliders*, eds. F.A. Harris et al., (World Scientific, Singapore, 1993), p.72.

[2] M. Jeżabek, Nucl. Phys. B (Proc. Suppl.) 37B (1994) 197.

[3] M. Woods, *Polarization at SLAC*, to appear in the proceedings of XI International Symposium on High Energy Spin Physics, SPIN'94, Sept.15-22, 1994, Bloomington, Indiana, USA.

[4] P.M. Zerwas (ed.), e^+e^- Collisions at 500 GeV: The Physics Potential, DESY Orange Reports DESY 92-123A, DESY 92-123B and DESY 93-123C.

[5] V.S. Fadin, V.A. Khoze and M.I. Kotsky, Z. Phys. C64 (1994) 45.

[6] M. Jeżabek, talk presented at XI International Symposium on High Energy Spin Physics, SPIN'94, Sept.15-22, 1994, Bloomington, Indiana, USA; R. Harlander, M. Jeżabek, J.H. Kühn and T. Teubner, *Polarization in Top*

Quark Production and Decay, to appear in the proceedings; preprint TTP 94-24, Karlsruhe, Nov. 1994, hep-ph/9411371.

[7] J.H. Kühn, A. Reiter and P.M. Zerwas, Nucl. Phys. B272 (1986) 560.

[8] M. Ježabek and J.H. Kühn, Nucl. Phys. B320 (1989) 20.

[9] A. Czarnecki, M. Ježabek and J.H. Kühn, Nucl. Phys. B351 (1991) 70;
A. Czarnecki and M. Ježabek, Nucl. Phys. B427 (1994) 3.

[10] M. Ježabek and J.H. Kühn, Phys. Lett. B329 (1994) 317.

[11] G. Alexander et al. (eds.), *Polarization at LEP*, CERN 88-06, Geneva 1988.

[12] M. Ježabek and J.H. Kühn, Phys. Lett. B207 (1988) 91.

[13] R.H. Dalitz and G.R. Goldstein, Phys. Rev. D45 (1992) 1531;
T. Arens and L.M. Sehgal, Nucl. Phys. B393 (1993) 46.

[14] H. Murayama and Y. Sumino, Phys. Rev. D47 (1993) 82.

[15] V.S. Fadin and V.A. Khoze, JETP Lett. 46 (1987) 525; Sov. J. Nucl. Phys. 48 (1988) 309.

[16] J.M. Strassler and M.E. Peskin, Phys. Rev D43 (1991) 1500.

[17] Y. Sumino, K. Fujii, K. Hagiwara, H. Murayama and C.-K. Ng, Phys. Rev. D47 (1993) 56.

[18] M. Ježabek, J.H. Kühn and T. Teubner, Z. Phys. C56 (1992) 653.

[19] J.H. Kühn and P.M. Zerwas, Phys. Reports 167 (1988) 321.

[20] M. Ježabek and T. Teubner, Z. Phys. C59 (1993) 669.

[21] B. Grządkowski, P. Krawczyk, J.H. Kühn and R.G. Stuart, Nucl. Phys. B281 (1987) 18.

[22] R.H. Guth and J.H. Kühn, Nucl. Phys. B368 (1992) 38.

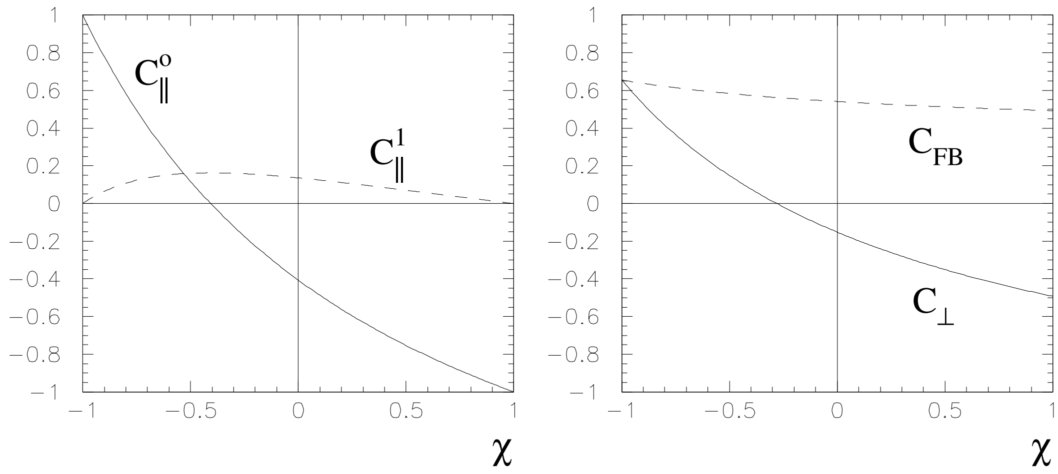

Figure 1: Coefficient functions: a) $C_\parallel^0(\chi)$ – solid line and $C_\parallel^1(\chi)$ – dashed line, b) $C_\perp(\chi)$ – solid line and $C_{FB}(\chi)$ – dashed line.

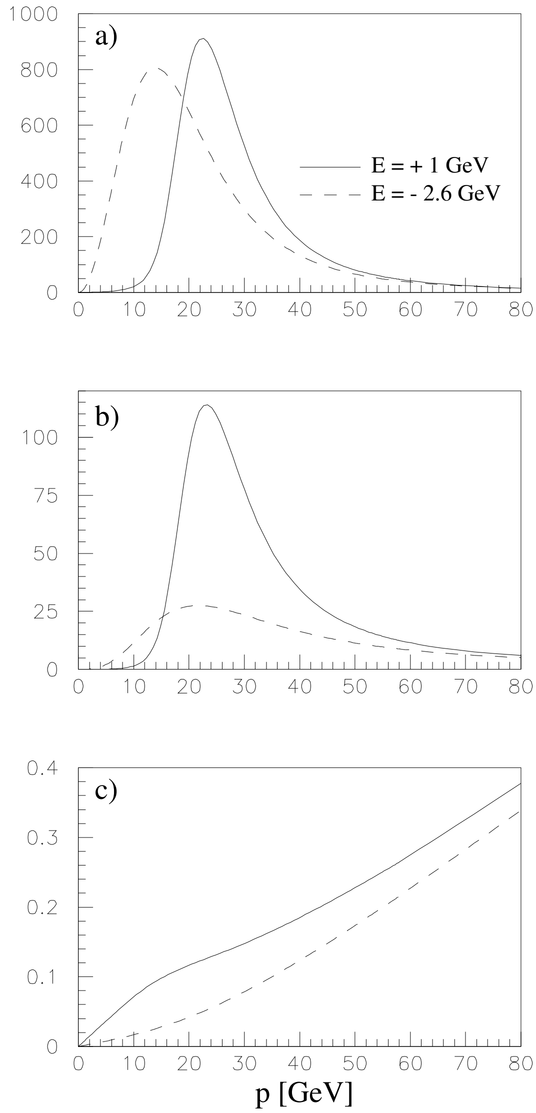

Figure 2: Momentum distributions: a) $\mathcal{D}_{S-S}(p,E)$, b) $\mathcal{D}_{S-P}(p,E)$, and c) their ratio $\varphi(p,E)$ for $E=1$ and $E=-2.6$ GeV – solid/dashed lines, $m_t=174$ GeV and $\alpha_s(m_Z)=0.12$.

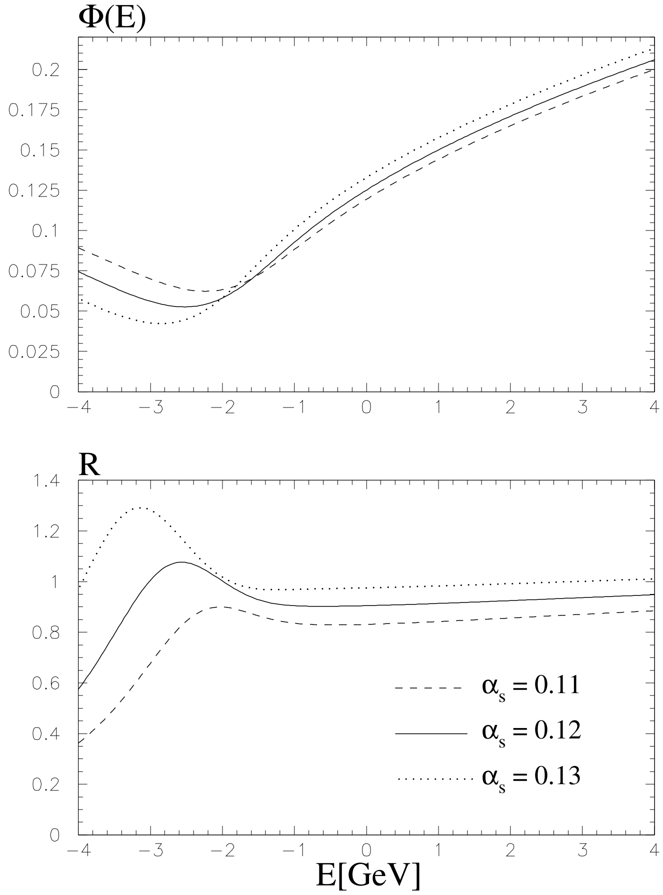

Figure 3: Energy dependence in the threshold region of: a) $\Phi(E)$ and b) $R = \sigma(e^+e^- \to t\bar{t})/\sigma(e^+e^- \to \mu^+\mu^-)$ for $m_t = 174$ GeV and $\alpha_s(m_Z) = 0.11$, 0.12 and 0.13 – dashed, solid and dotted lines, respectively.